

Computational sizing of solar powered peanut oil extraction in Senegal using a synthetic load profile

Wiomou Joévin Bonzi^{a,*}, Sebastian Romuli^a, Djicknoum Diouf^b, Bruno Piriou^c, Klaus Meissner^a, Joachim Müller^a

^a University of Hohenheim, Institute of Agricultural Engineering, Tropics and Subtropics Group, Stuttgart, Germany

^b Gaston Berger University, Faculty of Applied Sciences and Technology, Dept. of Applied Physics, Saint-Louis, Senegal

^c CIRAD, UPR BioWooEB, Montpellier, France

ARTICLE INFO

Keywords:

Feasibility study
HOMER Pro
Hybrid system
Mechanical pressing
Monte Carlo simulation
Plant oil

ABSTRACT

This paper presents an approach for sizing a hybrid photovoltaic system for a small-scale peanut oil processing company (Yaye Aissatou, Passy) in rural Senegal using a synthetic load profile. In this study, a predictive model of the electrical load of a service-based plant oil processing company was developed through a diagnosis, to evaluate the extraction process. The mass and energy balance were measured, and the process was implemented into MATLAB Simulink. The simulated load profile was implemented in HOMER Pro and the characteristics of the most profitable hybrid systems were identified. The results showed that the lowest net present cost over 25 years was found with a PV/battery/grid-system with 18.6 kW_p solar panels, 16 kWh of storage, and an initial investment of 20,019 €. Compared to a grid-only scenario, this solution reduces the net present cost from an initial 72,163 € to 31,603 €, the operating cost from 3675 € per year to 590 € per year, and the cost of energy from 0.29 to 0.13 €/kWh. The renewable fraction of the proposed system is 90.0 % while the expected payback period is 6.2 years. The study demonstrates the economic feasibility of using solar energy for plant oil processing.

Introduction

Electrifying small-scale industrial facilities in developing countries presents distinctive challenges and opportunities, specifically in the integration of renewable energy sources. Access to energy is one of the most important current challenges for developing countries. By 2030, 1.2 billion people in the world, mainly in Sub-Saharan Africa, with 85 % of them in rural areas will lack access to electricity (Kaygusuz, 2012). To enhance economic and social development, electricity should be more affordable and reliable. Renewable energy is presented as a solution to improve energy access. It provides an answer to two issues: local energy supply on one hand, and sustainable development on the other hand. Photovoltaics (PV) is one of the fastest-growing industries in the world and is well spread in sub-Saharan countries. It presents today several possible applications to face energy challenges (Parida et al., 2011). During the last decades, the price of PV cells has significantly decreased, and solar energy is now considered cheaper than fossil energy (Green, 2019).

PV systems can be classified as either on-grid or off-grid installations. While on-grid solutions can help mitigate grid failures and instability and reduce dependency, off-grid installations are standalone systems ideal for rural areas without access to the grid (Hernández-Callejo et al., 2019). However, they require more investment for storage capacity.

In addition to meeting household energy needs, energy plays a crucial role in supporting productive activities, particularly within the agricultural sector. The use of solar energy for productive purposes encompasses a range of applications, including cultivation, irrigation, post-harvest processing, and storage (Mandelli, Barbieri, et al., 2016). These applications often involve different types of photovoltaic (PV) systems. Firstly, standalone systems are tailored to specific machines, typically serving low-power applications in rural areas. Various turnkey solutions for such solar systems are described in literature, which are dedicated to productive use (Lighting Global, 2019; Olk & Mundt, 2016). Secondly, mini-grid systems are considered, accommodating diverse energy demands within a community. Given the prevalent energy access limitations in developing countries, studies on PV sizing

* Corresponding author at: University of Hohenheim, Institute of Agricultural Engineering, Tropics and Subtropics Group, Garbenstr. 9, 70599 Stuttgart, Germany.
E-mail addresses: bonzi.wiomoujoevin@uni-hohenheim.de, info440e@uni-hohenheim.de (W.J. Bonzi), sebastian_romuli@uni-hohenheim.de (S. Romuli), djicknoum.diouf@ugb.edu.sn (D. Diouf), bruno.piriou@cirad.fr (B. Piriou), klaus.meissner@uni-hohenheim.de (K. Meissner), joachim.mueller@uni-hohenheim.de (J. Müller).

<https://doi.org/10.1016/j.esd.2024.101391>

Received 18 November 2023; Received in revised form 21 January 2024; Accepted 22 January 2024

Available online 1 February 2024

0973-0826/© 2024 The Authors. Published by Elsevier Inc. on behalf of International Energy Initiative. This is an open access article under the CC BY license (<http://creativecommons.org/licenses/by/4.0/>).

primarily focus on mini-grid implementations, addressing the varied energy needs of households, businesses, public services, and small industries. (Gelchu et al., 2023; Harish et al., 2022; Mandelli, Brivio, et al., 2016; Wassie & Ahlgren, 2023). Lastly, there are systems tailored for higher-capacity industries. Studies have evaluated the feasibility of PV systems for industries, using analytical methods and relying on load profile models derived from interviews or electricity bills (Duma et al., 2023; Eales et al., 2017; Kumra et al., 2012; Thomas et al., 2014).

To be profitable, a sizing approach that considers energy generation capacity and economic aspect should be employed. Different approaches exist for sizing a PV system. Mathew et al. (2022) made a classification of the sizing optimization approaches and shows 12 categories including the conventional ones. Those are the analytical method, the numerical method, the probabilistic method, the intuitive method, and the deterministic method (Anoune et al., 2018; Barra et al., 1984; Khatib et al., 2016; Maghraby et al., 2002; Mellit, 2007; Sadio et al., 2018; Senthil Kumar et al., 2015). More recently, the artificial intelligence method is been used as alternative (Mellit et al., 2009). Moreover, a combination of two or more of these approaches can be carried out.

Several PV software tools exist, each with different specificities. They can be classified into four groups. The simulation tools simulate and predict the performances of a specified power system. The economics evaluation tools include an economic analysis of the system. The planning and analysis tools help in planning, designing, and optimizing different energy sources, and finally, the solar radiation maps are used for a good understanding of solar resources over the world (Alsadi & Khatib, 2018). Lalwani et al. (2010) investigated 12 major solar PV software and evaluated them according to their availability, cost, platform, capacity, and scope. Additionally, predictive models for PV systems exist and are used in software. The authors in (Rajesh & Carolin Mabel, 2015) present a review of existing models, with a state-of-the-art approach using artificial neural networks (ANN). Further research shows a review of the existing models and did a comparison between the most commonly used models in MATLAB, PVsyst and INSEL software (Ma et al., 2014). The software hybrid optimization model for electric renewables (HOMER) simulates grid-connected and standalone systems combined with other energy sources and performs optimization and sensitivity analysis, to find the optimal combination from a cost perspective. It is among the most commonly used software for PV sizing, and the most suitable for hybrid configuration (Awan et al., 2022; Bimenyimana et al., 2018, 2019; Lambert et al., 2005; Makkiabadi et al., 2021; Mathew et al., 2022; Oviroh & Jen, 2018; Rajesh & Carolin Mabel, 2015).

To find the ideal size of a PV system, an optimization problem must be solved based on various criteria, including location and meteorological data, electrical demand, technical considerations, economic considerations, reliability considerations, and environmental considerations (Khatib et al., 2016; Mathew et al., 2022). The meteorological data varies around the world, affecting the performance of a PV system. The electrical demand is characterized by the load profile, peak power, average consumption, and expected growth. A yearly load profile is necessary to evaluate the performance of a PV system throughout the year, with daily or hourly time steps. Thus, a smallest time step of the profile (minute or second), yields a more accurate optimization. The technical configuration of the system must meet the specifications of all components, with reliability being essential given the intermittent nature of solar energy. For critical weather conditions, a PV system can be oversized to include a security margin to meet requirements. Depending on the type of application, a reliability factor is defined, with a higher factor required for telecommunications, and a reduced factor for rural households. To minimize costs and consider revenue, the budget, installation, maintenance and operation costs, and replacement cost should be minimized, with energy selling revenue expected to be considered. Additionally, environmental impact should be mitigated. (Mathew et al., 2022).

Understanding the load profile is then essential for PV sizing. This

can be achieved through long- or short-term measurements or predictions (Serrano-Guerrero et al., 2018). Previous studies present models for energy profiles prediction based on consumer parameters, or employing surveys, regression analysis, decision trees, and ANN (Abarkan et al., 2013; Blodgett et al., 2017; Lorenzoni et al., 2020; Serrano-Guerrero et al., 2018; Tso & Yau, 2007). ANN has been successful in forecasting household electric energy consumption and load profiles (Rodrigues et al., 2014). Moreover, authors in (Chuan & Ukil, 2015; Sepehr et al., 2018) propose a mathematical model to predict the random behaviour of residential buildings in energy consumption based on a bottom-up approach.

The bottom-up approach is commonly used in the literature to simulate household electricity consumption and has proven its reliability (Sepehr et al., 2018). Its principle is to construct the total load profile from the profiles of elementary components, which can be a household or a single electrical device, depending on the objective. This approach allows for the analysis of the effect of the operation of elementary equipment on the total load profile. Ogwumike et al. (2013) made a model on MATLAB Simulink of the profile of a residential load profile and perform an optimization on the scheduling appliances to minimize the costs of electricity. Some studies present standardized load profiles for domestic or industrial applications, such as (Gouveia & Seixas, 2016; Sanchez et al., 2009) which use segmentation to determine similarities in household load profiles. Sandhaas et al. (2022) developed a model generating synthetic load profiles for 11 industry types based on the normalised load profiles of eight electrical end use applications. However, the study is related to German industry. Little and Blanchard (2022) assessed various productive uses of energy in Tanzania through business surveys and literature to define their load profiles. Nevertheless, their findings are limited to small-scale applications and do not apply to industries with multiple overlapping equipment. Latest versions of HOMER software have a standard profile for commercial, industrial or household activities. Unfortunately, most studies that evaluated load profiles focus on households (Wijaya & Tezuka, 2013), while the few examples that examined industrial activities are not relevant to small and medium-sized enterprises (SME) in rural areas, especially in West Africa. Furthermore, the sizing conducted for industries in developing countries relies on load profiles derived from interviews and electrical bills.

In this study, the objective was to design a tailor-made hybrid PV solution for a typical small peanut oil processing SME in Senegal. A bottom-up approach was used to simulate the load profile on MATLAB Simulink, considering the variability of customers. The resulting load profile was used in the HOMER Pro software to size a PV system.

Materials and methods

Material

Location

This study focused on evaluating a peanut oil production SME located in Passy, Senegal (13°58'47.4"N 16°15'36.5"W). The SME has 306 m² of available space, with 57 % being roofed. The diagnosis was conducted during the dry season (April) under typical production conditions. The main activity is the processing of peanut seeds into edible oil, on a service basis. Customers bring their peanuts to the site for processing and pay based on the number of oil bottles filled and the amount of press cake taken home. During the peanut oil production season, from October to May, the demand for processing services is very high, with workdays often extended until 23:00, resulting in almost 16 h of operation per day. The SME had an average capacity of 4 tons per day of processed in-shell peanuts.

Raw material

In-shell peanuts were used as raw material for the production of peanut oil in the SME. It is packed in 50 kg bags when the customers are

arriving at the SME. About 2 kg of raw material was collected and transported for further analysis to the laboratory at the University of Hohenheim (Stuttgart, Germany). A water content of 3.7 % d.b. and an oil content of 49.0 % d.b. were determined according to (CEN/TS 14774-3:2004, 2004) and (DGF-Einheitsmethoden, 2006) in three repetitions.

Process description

The site is equipped with two shellers, six steamers, three presses and a filter. On-site measurements were conducted during operation to determine electrical consumption, material throughput, process efficiency, and duration of each equipment. The equipment is listed in Table 1.

The process begins with the in-shell peanuts being shelled using one of the two available shellers. The resulting kernels are then sent for steam treatment in one of the available steamers. The recovered shells are either reused in the steamers' burner or mixed with the steamed kernels for pressing at a later time. The steaming is done in batches of approximately 80 kg and takes around 1.5 h to be completed. Once steamed, the kernels are mixed with 15 % of shells and pressed in one of the available presses. The shells are added to form microchannels in the cake to support the flow of oil. The crude oil obtained from the oil press is then filtered using a plate filter with an associated pump (Fig. 1).

Method

On-site measurement

During two subsequent days in April 2022, on-site measurements were conducted to complete a mass balance of each unit operation. As the daily routine is the same throughout the season, several processing batches were monitored as a baseline for simulating the entire production year. The energy requirement of each unit operation was measured through the average electrical power of the operation engine. Several batches of the process were followed to evaluate the mass flow of each operation. The material before and after each operation was weighed using a weighing tray with a precision of 1 kg and the durations of the operations were monitored. This allowed for the calculation of the operation throughputs and the operation efficiencies. Samples of each by-product were taken for laboratory analyses. Electrical power was measured with a current clamp (testo 770-3, Testo SE & Co. KGaA, Dubai, United Arab Emirates) associated with a data logger (testo 400, Testo SE & Co. KGaA, Dubai, United Arab Emirates). Additional information on the SME's mode of operation, average daily production, and average daily electricity consumption were obtained through interviews. The daily average production and energy consumption were used later in the model optimization to determine customer arrival parameters.

Modeling load profiles

MATLAB Simulink 10.5 (MathWorks®, Natick, Massachusetts, USA) was utilized to simulate the peanut oil production process and evaluate the electric load. The Simulink block model is illustrated in Fig. 2, comprising five main blocks: material receipt, shelling, steaming, oil pressing, and filtration. The model operates on a minute-by-minute basis, evaluating energy consumption and productivity over a year.

In a service-oriented industry dependent on customers, raw material

availability limits the production. The simulation starts with the material receipt block, and computes in-shell peanut mass. The operation strategy is defined through three major parameters affecting the operations commands: (i) the randomly arriving customers, (ii) the weekly schedule with start and stop times as well as weekends and (iii) the typical months which represents the production season. In order to account for the randomness of activities, parameters such as the maximum order size per customer, the customer arrival probability, and the customer acceptance time window were taken into consideration. Moving forward, the shelling, steaming, oil pressing, and filtration blocks share a similar configuration. Depending on customer demand, multiple operations may be carried out simultaneously. The applied approach relies on a mass balance of the entire process to understand when and how an operation runs. The calculations involve parameters such as output from the preceding operation, process efficiency, throughput, and average power. Operations commence when the batch of the previous operation is completed and supplied to the current one. For instance, if a customer's batch of peanuts is fully pressed, the resulting crude oil quantity is supplied to the filtration block. This process continues until the supplied quantity is fully processed. At every time step, the electrical power of each operation is added to the load profile.

The simulation model was implemented with a set of algorithms, starting with the material receipt:

$$m_i = CAI_i \times n_i \times 50 \quad (1)$$

where m_i (kg) is the mass of the receipted in-shell peanut in the SME at a time step i , CAI_i is the customer arrival indicator (1 if a customer arrives, 0 otherwise), and n_i is the order size as an integer in a range of 1 to n_{max} . n_{max} indicates the maximum number of 50-kg-bags of in-shell peanuts, that a customer can bring to the SME for processing at any given time. The probability of a new customer arriving at the SME for processing within a 10-minute-interval during the acceptance window is expressed as:

$$P(CAI_i) = \begin{cases} p_c, & CAI_i = 1 \\ 1 - p_c, & CAI_i = 0 \end{cases} \quad (2)$$

where p_c is the customer arrival probability. The time interval is denoted as $i \in [T_{start}, T_{end}]$, representing the customer acceptance window. T_{start} is the time at which the SME begins accepting customers and their material for processing while T_{end} is the time at which the SME stops accepting customers.

The shelling, steaming, oil pressing, and filtration blocks share the same configuration.

The instant power was calculated as

$$P_{k,i} = C_{k,i} \times P_k \quad (3)$$

The peak power when the engine start was integrated by a multiple n as:

$$P_{k,i} = r \times C_{k,i} \times P_k \text{ if } P_{k,i-1} = 0 \quad (4)$$

where $P_{k,i}$ (W) is the instant power of the operation k at a time step i , r is the peak to average power ratio, $C_{k,i}$ is the command from the operation strategy, and P_k (W) the averaged electrical power of the operation k engine. $C_{k,i}$ is taking the value 0 when the operation k is running and 1 otherwise. The values of r and P_k are obtained through field measurement and considered constant.

The throughput of transformed product $TP_{k,i}$ was expressed as follow:

$$TP_{k,i} = C_{k,i} \times Eff_k \times TP_k \quad (5)$$

where $TP_{k,i}$ (kg/min) is the throughput of processed material of operation k at a time step i , TP_k (kg/min) is the average throughput of processed material of operation k and Eff_k (kg/kg) is the transformed product per kg of raw material, i.e. the operation yield. TP_k and Eff_k have

Table 1

List of equipment used in the peanut oil extraction SME in Passy, Senegal.

Equipment	Type	Origin
Shellers 1 + 2	Blowers and rotating cages	Local
Steamers 1 – 6	Cylinder on rocket stove	Local
Oil press 1 + 2	Screw press, extraction at the near end of the screw	China
Oil press 3	Screw press, extraction at the far end of the screw	China
Filter	Plate filter	China

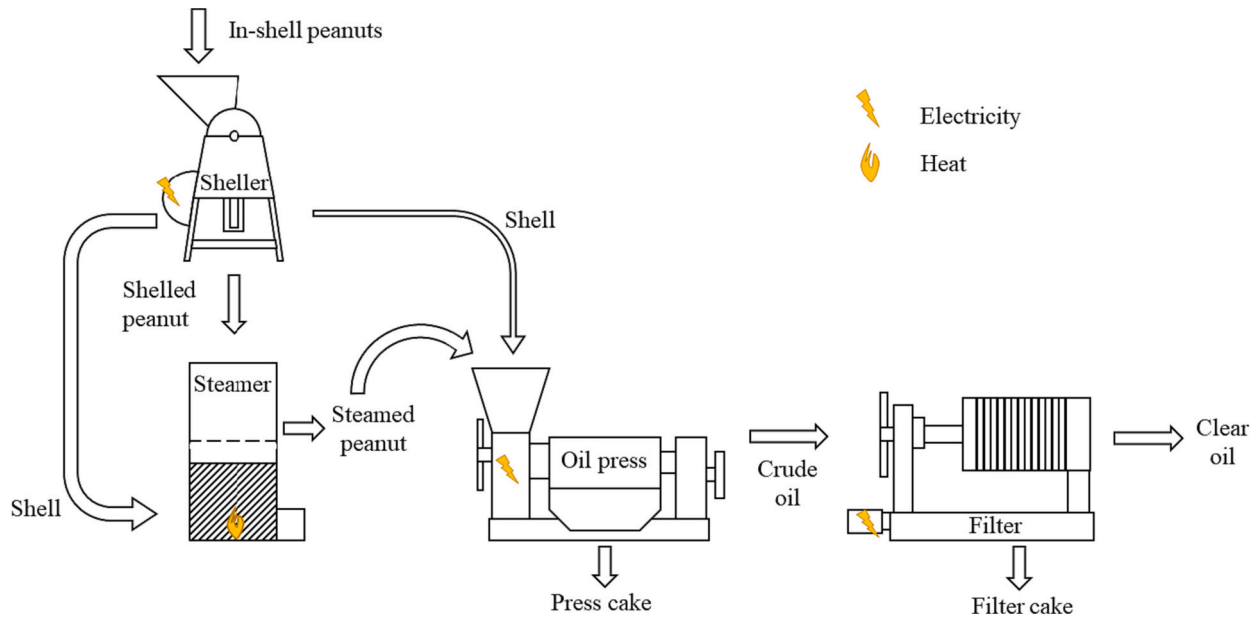


Fig. 1. Unit operation in the peanut oil production process.

Abbreviation	Parameter
m	Raw material
TPSh	Throughput of sheller
P_Sh	Electrical power of sheller
TPS	Throughput of steamer
TPOil	Throughput of oil press
P_Oil	Electrical power of oil press
TPFP	Throughput of filter press
P_FP	Electrical power of filter press

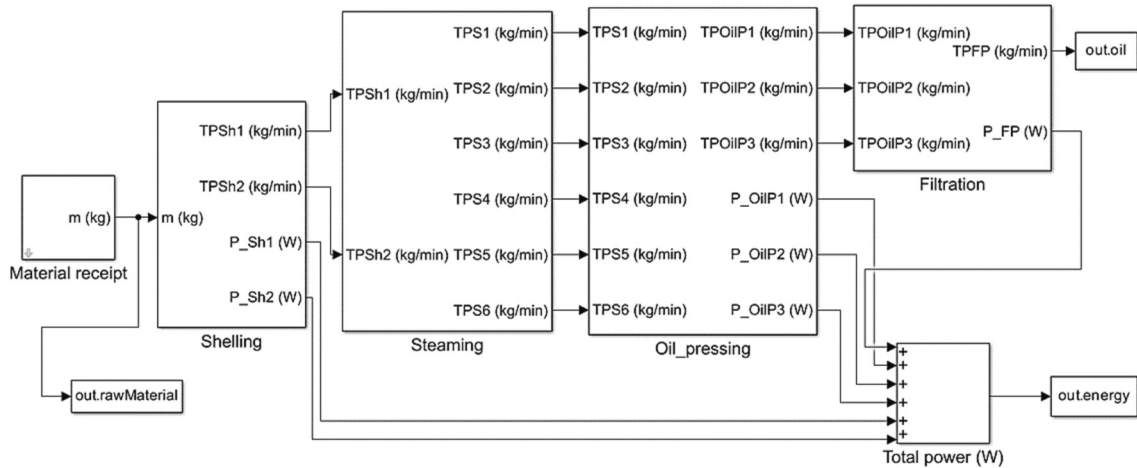


Fig. 2. Peanut oil process Simulink block model.

been calculated by tracking several batches during the diagnosis of the SME and are considered constant throughout the operation.

The transformed material in an operation is stored temporarily before going to the next operation when the next engine will be free for usage. This is done in the SME since the batches are for customers and should not mix with each other. The intermediate storage is given by:

$$S_{k,i} = \sum_{t=0}^i T p_{k-1,t} - \frac{T p_{k,i}}{Eff_k} \quad (6)$$

where $S_{k,i}$ (kg) is the material from the operation $k-1$ stored before operation k , a time step i .

The model simulates each minute of the operation as shown in Fig. 3. The energy consumption E is given by:

$$E = \frac{1}{60} \sum_{i=0}^T \left(\sum_k P_{k,i} \right) \quad (7)$$

where E (Wh) is the total energy consumption of the SME and T (min) is the duration of the simulation. The simulation monitored the electrical load of individual operation $P_{k,i}$, the total load $\sum P_{k,i}$, and the productivity on a one-minute basis for a duration of one year. The details of the content of the simulation blocks are included in Appendix B.

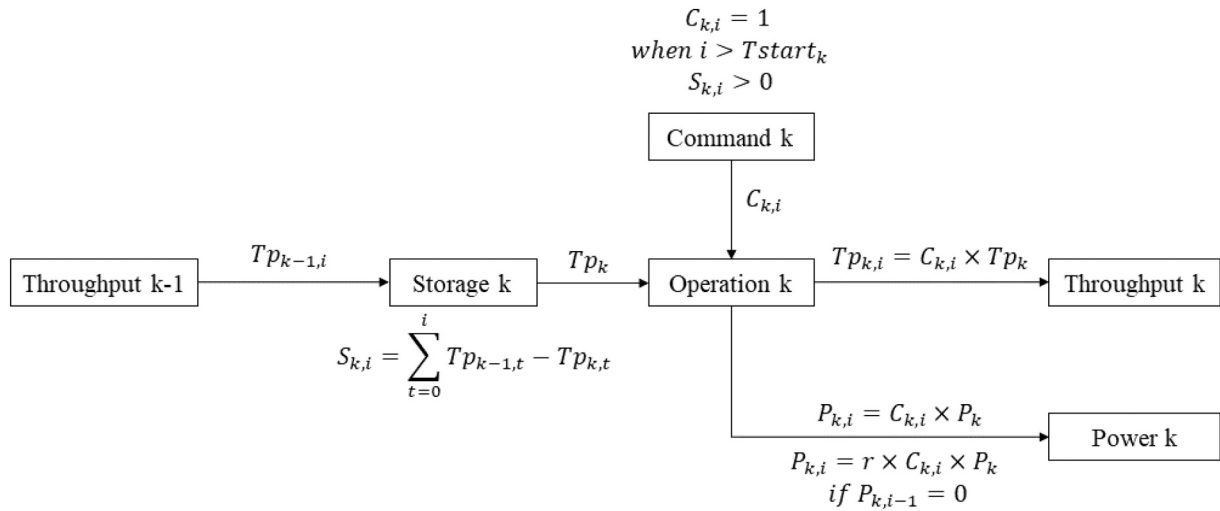


Fig. 3. Operation block mathematical model, where $Tstart_k$ is the time at which operation k can start.

Sensitivity analysis

In the established model, measures have been taken to define the operating parameters of each machine. Remaining parameters, including the customer acceptance window, arrival probability, and order size, were subject to determination. To determine the parameters values corresponding to the SME, a Monte Carlo simulation was conducted. The customer acceptance start time was set at 6:00 and the acceptance windows was controlled by the end time of acceptance. The considered variables in the analysis are shown in Table 2. The results of the study were used to determine the parameters corresponding to the 4 tons of processed in-shell peanuts per day at 67 kWh per day. An optimization algorithm minimizing the root mean square error (RMSE) was used on the MATLAB Simulink parameter estimator. The Fig. 4 shows the parameters adjusted in the optimization to obtain the targeted productivity and energy consumption.

Load profile validation

A k-means clustering algorithm was applied using Statistical Analysis System (SAS) 9.4 (SAS Institute Inc., Cary, NC) to categorize simulated and measured power profiles into distinct centroids and capture variations in average power levels and their occurrences. The k-means is a non-hierarchical cluster algorithm that has been applied in several domains, including load profile classification and equipment identification (Azad et al., 2014; Ikotun et al., 2023; G. Zhang et al., 2020). The k-means clustering classified the load profiles values into k clusters around centroids. For validation, a statistical comparison between on-site measurements and simulations was made using the Normalised Root Mean Squared Error (NRMSE) given by:

$$NRMSE = \frac{\sqrt{\sum_x^N (P_{model,x} - P_{measured,x})^2}}{P_{measured,average}} \quad (8)$$

where $P_{model,x}$ (W) is a centroid of the simulation load, $P_{measured,x}$ (W) is the related measured centroid, N is the number of centroids, and $P_{measured, average}$ is the averaged mean power (W). The power mean values,

Table 2

Parameters for sensitivity analysis on load profile.

Parameter	Unit	Lower value	Upper value
End time of customer acceptance, T_{end}	hh:mm	10:00	20:00
Customer arrival probability, p_c		0	1
Maximum order size per customer, n_{max}	50-kg-bag	1	10

standard deviation, power peak, and load factor are provided for both simulated and measured profiles over one simulated year and two days of on-site measurements. The load factor (LF) is calculated by:

$$LF = \frac{P_{average}}{P_{peak}} \quad (9)$$

where $P_{average}$ (W) is the load average power, and P_{peak} (W) is the daily peak power.

PV sizing

HOMER Pro 3.14.2 (UL Solutions, Boulder Colorado, USA) was used to determine the optimal size and combination of a hybrid system, as depicted in Fig. 5. The microgrid components considered were based on generic components provided by the HOMER library, but were modified to match the available components in Senegal. The energy sources were the grid, a diesel generator, and PV panels. The monthly average solar global horizontal irradiance (GHI) was determined using data from NASA Prediction of Worldwide Energy Resource (Jul 1983 – Jun 2005) (Zhang et al., 2008) considering the SME location. The average daily radiation ranged from a minimum of 4.92 kWh/m²/day in December to a maximum of 7.07 kWh/m²/day in April. The generic flat plate PV component was selected from the HOMER library with an efficiency of 17 % at standard test conditions. A derating factor of 80 % and a lifetime of 25 years have been considered. The installation assumed no tracking, placing the PV at the ideal slope (14.0°) and azimuth (0°) for the location. Opting for effective storage longevity, the generic 1 kWh Li-Ion battery was chosen from the library. It features a round trip efficiency of 90 %, a minimum State of Charge (SOC) of 20 %, and a throughput of 3000 kWh with a 15-year float life. As for the inverter, the generic System Converter was chosen with an efficiency of 95 % and a lifespan of 15 years. Finally, the auto-size Genset was utilized as the generator, with a minimum load ratio of 25 % and a lifespan of 15,000 h. Two dispatch strategies, Load Following (LFS) and Cycle Charging (CCS), were assessed in the simulation, both involving the generator operating whenever the renewable source is insufficient. In LFS, the generator produces sufficient power to meet the load, while in CCS, it operates at full capacity to fulfill the load and charge the battery to 80 %. The optimal strategy was chosen for each scenario. In the presented results, the off grid scenario with the generator utilized CCS, while the other scenarios with generator utilized LFS.

All hybrid scenarios combining one or more of these energy sources, with or without a battery, were evaluated. Thus, a renewable solution is made up solely of PV panels, with or without battery storage. A grid-connected solution includes the grid, while an off-grid solution

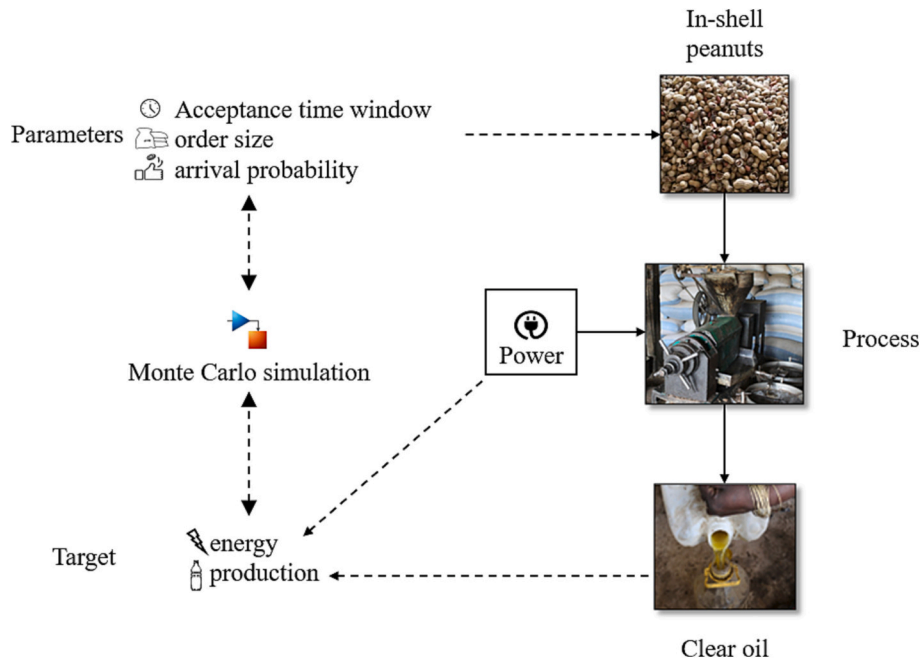


Fig. 4. Peanut oil process simulated in Simulink and optimization approach.

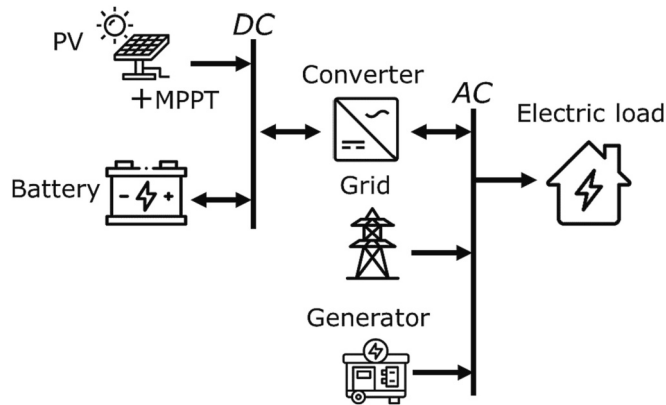


Fig. 5. Configuration of hybrid system combinations using HOMER Pro.

excludes it. The scenarios are represented by codes including their energy sources such as PV/battery/grid/diesel. Out of 14 possible combinations, four were excluded: the PV-only option was not technically feasible and the diesel-only, PV/diesel, and battery/diesel scenarios were extremely expensive.

Randomized grid outages were considered in the simulation. For Senegal a mean outage frequency of 19 days per year with a mean repair time of one hour was considered based on data from the World Bank (2019).

For all scenarios, a project lifetime of 25 years, a discount rate of 4.5 %, and an inflation rate of 2.5 % were used. The individual costs of solar component, replacement, and operation and maintenance costs were based on an interview with a solar company (ENERGECO, Dakar, Senegal). The economic parameters included in HOMER Pro are shown in Table 3. The differences in costs between the installation and replacement of the PV, the battery, and the inverter correspond to the expenses associated with a roof support, accessory for battery installation, and connection accessories of the system, respectively.

During the simulation, various constraints were imposed in the optimization process. The maximum capacity shortage refers to a deficit in required operating capacity and the actual operating capacity the

Table 3

Economic parameters included in HOMER Pro.

Component	Capacity	Installation (€)	Replacement (€)	O&M ^a	
PV	1 kW _p	533.6	457.3	1.52	€/a
MPPT	1 kW _p	76.2	76.2		
Battery	1 kWh	297.9	206.4	0.76	€/a
Inverter	1 kW	457.3	152.4	1.52	€/a
Grid	1 kWh			0.29	€/kWh
Diesel generator	1 kW	167.7	167.7	1.00; 0.53	€/L ^b ; €/h

^a O&M: Operation and Maintenance cost.

^b Diesel price.

system can deliver. For the current operation of the SME powered solely by the grid, the capacity shortage was evaluated at 0.4 % based on the load profile and the grid reliability. The maximum capacity shortage of the hybrid scenarios proposed was then limited to this value. A lower value would require combining the grid with another energy source to meet the energy needs, while a higher capacity shortage could result in using a less reliable renewable energy source. No limit was set on the amount of renewable energy that can be used. The primary objective is to identify the most cost-effective solution that results in the least net present cost (NPC) over the project lifetime. To ensure adequate operating reserves, a surcharge of 10 % (Halabi et al., 2017; Salehin et al., 2016) was set on the load profile, and one of 30 % on the solar power output (Vu & Chung, 2022).

Results

Diagnosis results

The diagnosis allowed to identify the parameters presented in Table 4, which were then used as inputs for the simulation model. The sensitivity analysis on the operation strategy parameters was conducted to match the daily production capacity of 4 tons.

The mass balance for producing one ton of clear oil is illustrated in Fig. 6 using a Sankey diagram. The diagram shows that the operation requires 4.4 tons of in-shell peanuts, out of which 1.7 tons of shells are

Table 4
Peanut oil production operation parameters.

Process	Device no.	Throughput (kg/min)	Operation yield (kg/kg)	Start time (hh: mm)	Power (W)
Shelling	1	7.9	0.6	06:00	1700
	2				1100
Steaming	1 – 4	1.5	1.1	06:00	
	5 + 6	0.9	1.1		
Pressing	1	1.8	0.4	06:00	2000
	2	1.8	0.4		1500
	3	3.3	0.4		4000
Filtration	1	4.5	0.9	06:00	900

used as fuel during the steaming process and mixed with the steamed peanuts. To steam the shelled peanuts, 156 kg of water is added, which increases the moisture content from 3.7 to 6.9 % d.b. Analysis shows a significant difference between the moisture content of shelled peanut, steamed peanut and press cake. After pressing, 1058 kg of crude oil is obtained, resulting in an operation yield of 37 %. The press cake produced has an oil content of 10.7 % d.b, and is significantly different from the oil content of the shelled and steamed peanut (49.0 and 48.6 %). It corresponds to an oil recovery of 87.3 %.

Estimation of electric power consumption

Simulated load profile

Fig. 7 displays the load profiles for a typical day of production, including the power usage of individual equipment and the total power consumption of the SME.

Fig. 8 depicts the simulated load profiles for a standard week and a standard year, respectively. These profiles vary from day to day due to the random effect of raw material arrival in the model. The period from May to September is considered as off-season.

Validation

Based on the simulation results, the following parameter values were identified: the customer acceptance window from 06:00 to 16:20, the maximum order size of 5 50-kg-bags, and the customer arrival probability of 0.69. Fig. 9 compares the simulated load profile of the three presses with the load profile measured on-site during 9 h of operation. The comparison was made by considering the total power consumption of the three oil presses present on-site. The different levels of operation, whether 1 press, 2 presses, or 3 presses are being used can be distinguished in the on-site measurement and the simulated load profile. The

peak loads during start-up were instantaneous and could hardly be captured by the measuring device.

The histograms in Fig. 10 show the different operating powers that correspond to the power of the three oil presses (P1), (P2), and (P3) and the combinations, when oil presses are used simultaneously because of high capacity demand. The simulation shows high counts at a power of 7500 W (P1–3) and 3500 W (P1 + 2) when respectively all of the three oil presses or when (P1) and (P2) are operated simultaneously. Medium counts at a power of 1500 W (P1) and 2000 W (P2) are also noticeable. Due to variabilities of the instant power of machinery during the on-site measurements, normal distributions of power counts are noticeable, however, centered around the operating points in the simulation. High counts in the measured power indicate the operation with two presses (P1 + 2), and all three presses (P1–3) similarly to the simulation. A k-means clustering classification determines eight centroids in the simulated and measured profiles, along with their frequency appearances. The analysis was performed on the data measured over two days, and the load profile simulated for one year. The results are presented in Table 5, and the calculation of the NRMSE for the centroids yields a value of 7.07 %.

A majority of the measured values (62 %) were concentrated around 3543 W (P1 + 2) and 7440 W (P1–3). Similarly, over half of the simulated values (58 %) were centered around 3505 W (P1 + 2) and 7510 W (P1–3). The centroid (P0) represents the power when no presses are in operation, with a measured value of approximately 34 W and a simulated value of 0 W. An additional centroid (PP) in the measured load can be attributed to the peak power of the equipment and occasional material overload, resulting in higher power requirements.

Statistical comparisons were made on both profiles. Although the confidence interval of the on-site measurements is wider than that of the simulation, the average power shows a similarity and the range of the on-site measurements includes the range of the simulations (Fig. 10). The mean values, standard deviation, power peak and load factor of the simulated and measured values are shown in Table 6.

Sensitivity analysis

The points considered as input in the sensitivity analysis are displayed in Fig. 11. It presents the effect of customer randomness on the daily productivity. The figure displays the total amount of in-shell peanut processed per day and the daily energy consumption, average power, and peak power. The histograms show the output of the simulation as frequency of occurrence of the response values simulation. The results show that the customer arrival probability is the most influential parameter on in-shell peanut processed, the energy consumed, and the peak power with a correlation coefficient (r) varying between 0.65 and

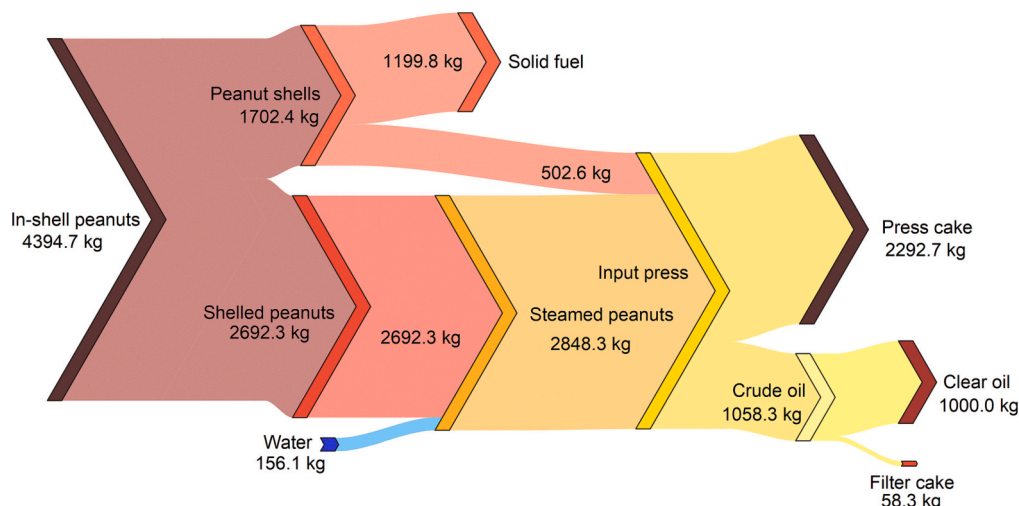


Fig. 6. Mass balance for the production of 1 ton of clear oil.

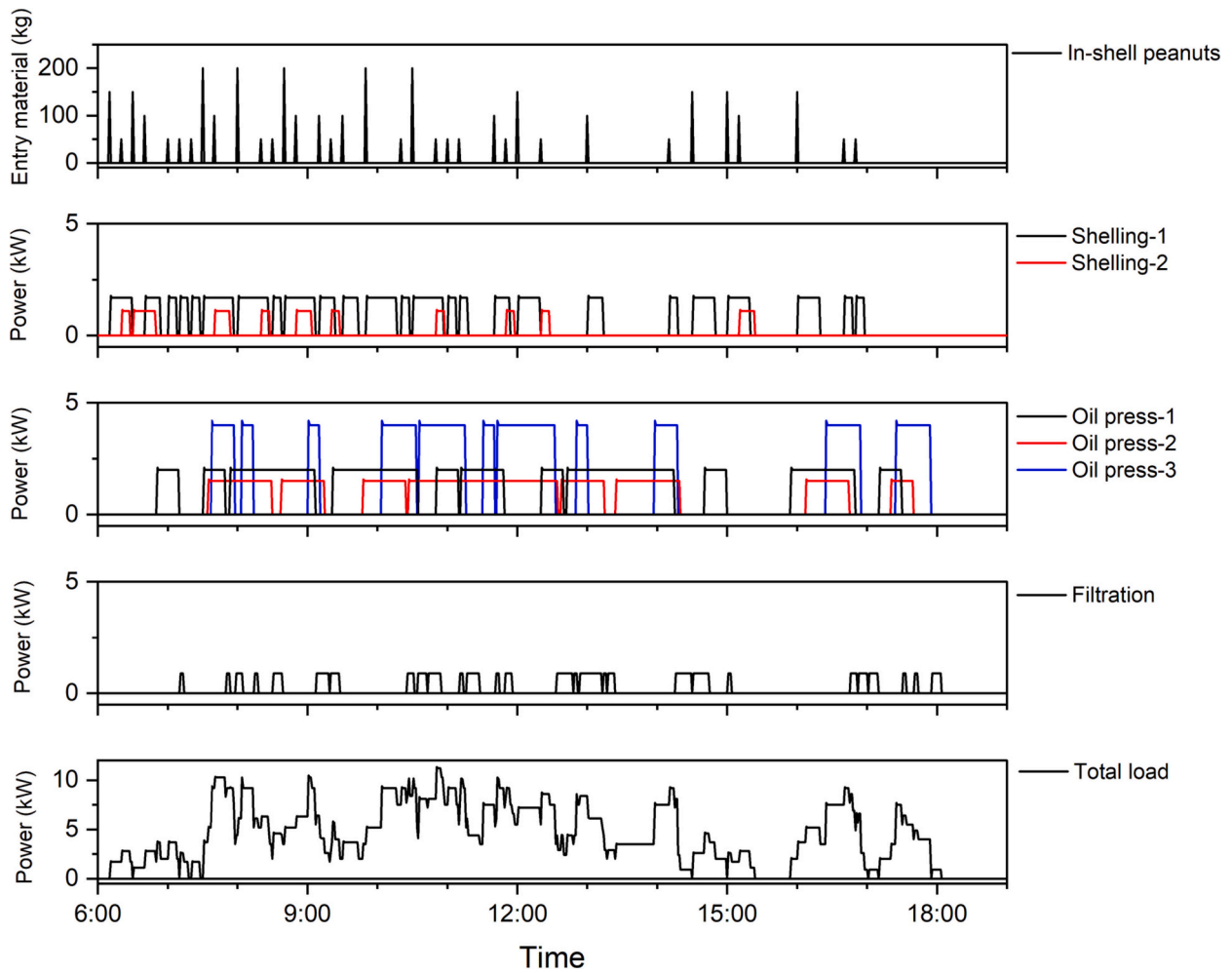


Fig. 7. Simulated daily load profile.

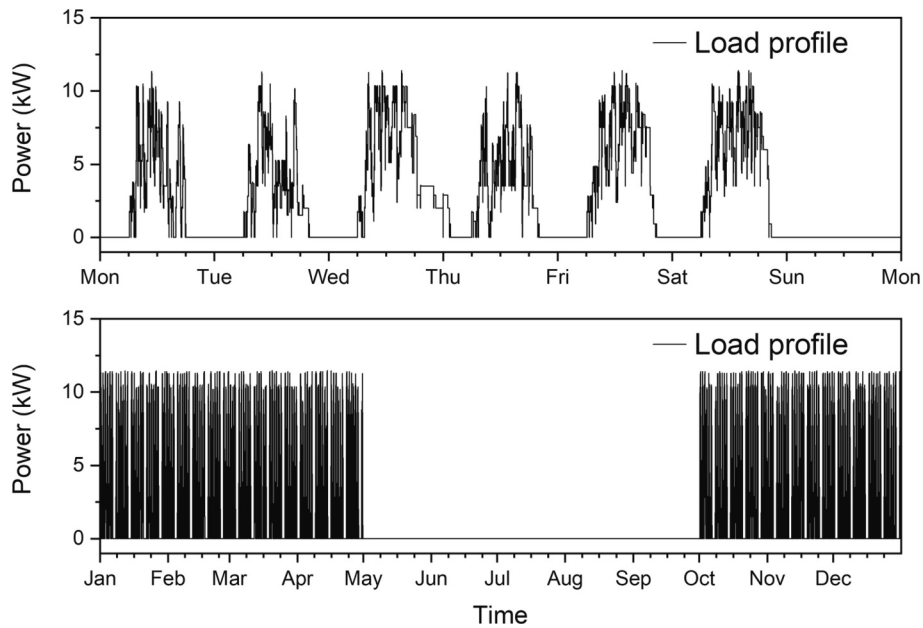


Fig. 8. Simulated week (top) and year (bottom) load profile.

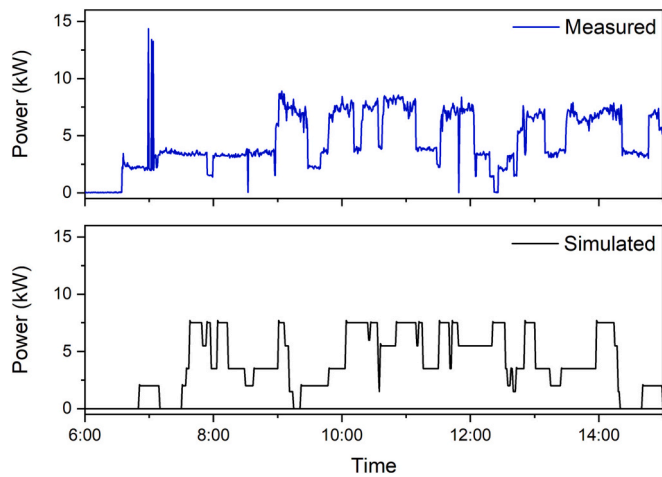


Fig. 9. Cumulated load profile of the oil presses, measured (top) and simulated (bottom).

0.76 with a p -value < 0.001 . A probability of at least 0.25 is necessary for the processing of four tons per day and energy consumption of 67 kWh. The maximum order size has a limiting impact on production, with at least four bags of 50 kg per customer to achieve the daily production of four tons.

Composition and sizing of power supply scenarios

Five main scenarios are presented in the following. Those are the base case scenario, and the best scenarios for a fully renewable system, a hybrid system, an off-grid system and a system without battery storage.

Grid-scenario

The grid-scenario is the current situation in the SME and represents the baseline scenario. It does not require an investment and operates solely with electricity from the grid. The cost of energy (COE) is set to 0.29 €/kWh, which is the actual price the SME is currently paying. The energy consumption of the SME operating with this scenario is 12,504 kWh/a, with a NPC of 72,163 €, representing 3675 €/a of energy cost. Due to grid outages, an unmet demand of 0.41 % is assumed in this scenario.

PV/battery-scenario

The PV/battery-scenario is a 100 % renewable energy system powered exclusively by PV. Since power is also needed after sunset, a storage system is needed, which is provided by a battery. The optimal configuration would consist of 46.6 kW_p of PV and a battery storage of 40 kWh. Fig. 12 illustrates one week of production for the PV/battery-scenario. It can be seen that on a sunny day, peak PV production could reach almost four times the demand. The daytime demand can be fulfilled while charging the battery even during cloudy days (Thursday and Friday in the example). The battery is also regularly called upon early in the morning when the SME start to operate at 6:00, and at sunset.

The NPC of the PV/battery-scenario would be 54,958 €, with an initial investment of 45,323 €, where 24,843 € is for PV and 11,916 € for the battery. The cost of energy (COE) would be 0.22 €/kWh. The energy

Table 6

Statistical comparison between measured and simulated power on a minute basis.

	Mean (W)	Standard deviation (W)	Peak power (W)	Load factor (%)
Simulated	4451	1896	7700	57.8
Measured	4808	2171	8910	54.0

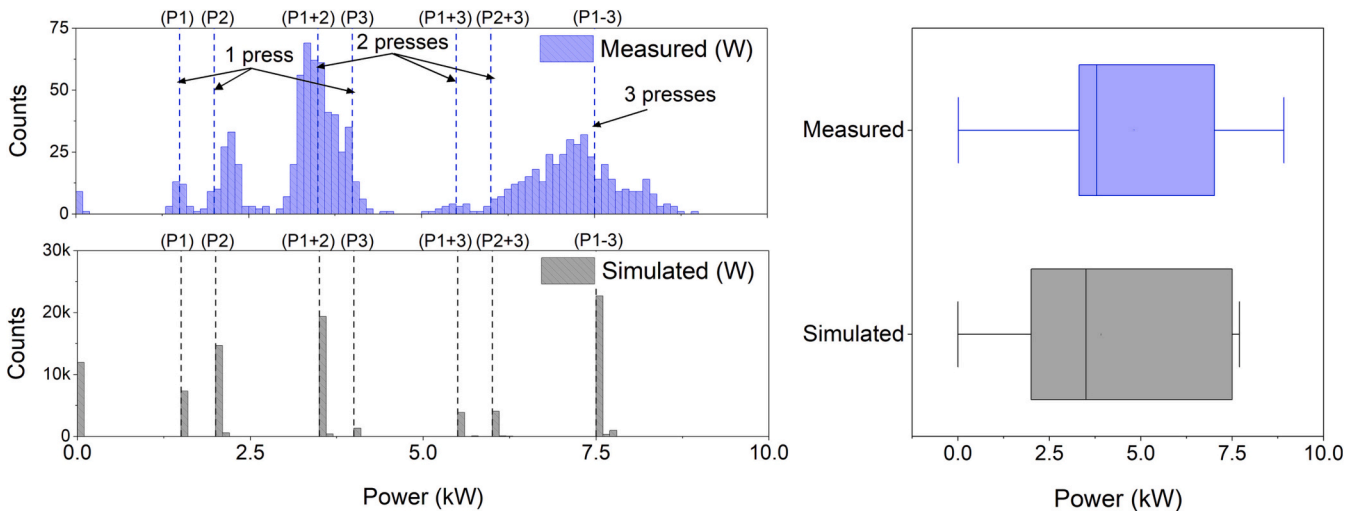


Fig. 10. Power profiles of on-site measurements and simulation (left) and box plot of average power demand (right).

Table 5

Load profiles centroids and frequency for measured and simulated power.

Load profile	Parameter	Centroids								
Equipment		(P0) ^a	(P1)	(P2)	(P1 + 2)	(P3)	(P1 + 3)	(P2 + 3)	(P1 - 3)	(PP) ^b
Measured	Power (W)	44	1574	2250	3543		5529	6660	7440	8290
	Frequency (%)		4 %	11 %	44 %		3 %	16 %	18 %	5 %
Simulated	Power (W)	0	1500	2004	3505	4000	5503	6004	7510	
	Frequency (%)		10 %	20 %	26 %	2 %	5 %	5 %	32 %	

^a (P0): no-load power.

^b (PP): peak power.

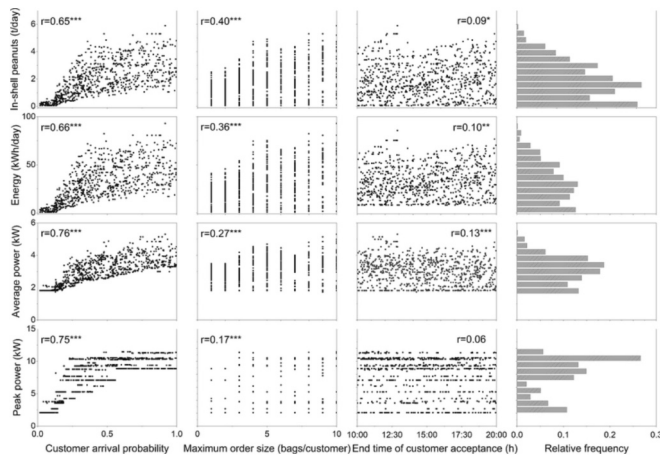


Fig. 11. Monte Carlo simulation results for sensitivity analysis and correlation coefficient; *significant at 0.05 level, **significant at 0.01 level or lower, ***significant at 0.001 level or lower.

surplus would be very high with 62,961 kWh/a (82.5 %), since the system has to be oversized to provide enough energy during unfavourable weather condition.

PV/battery/diesel-scenario

The PV/battery/diesel-scenario is a PV/battery system combined with a diesel generator in order to avoid the oversizing that would be necessary for operation in days of low solar radiation. It corresponds to the best off-grid scenario. The system would consist of 24.5 kW_p of PV with a storage capacity of 40 kWh combined with a diesel generator supporting only 4.1 % of the energy demand.

Fig. 13 illustrates one week of production for the PV/battery/diesel-scenario. On sunny days, PV power is double the demand (Tuesday, Wednesday and Saturday). This allows to charge the battery while covering the daytime demand. The battery is used in the morning and at sunset. On cloudy days, diesel is used to fulfill the demand and quickly charge the battery (Monday, Thursday and Friday). It should be noted, that the generator produces more than necessary, as it is sized to cover the SME's maximum requirements unlike the battery, which only supplies the actual demand.

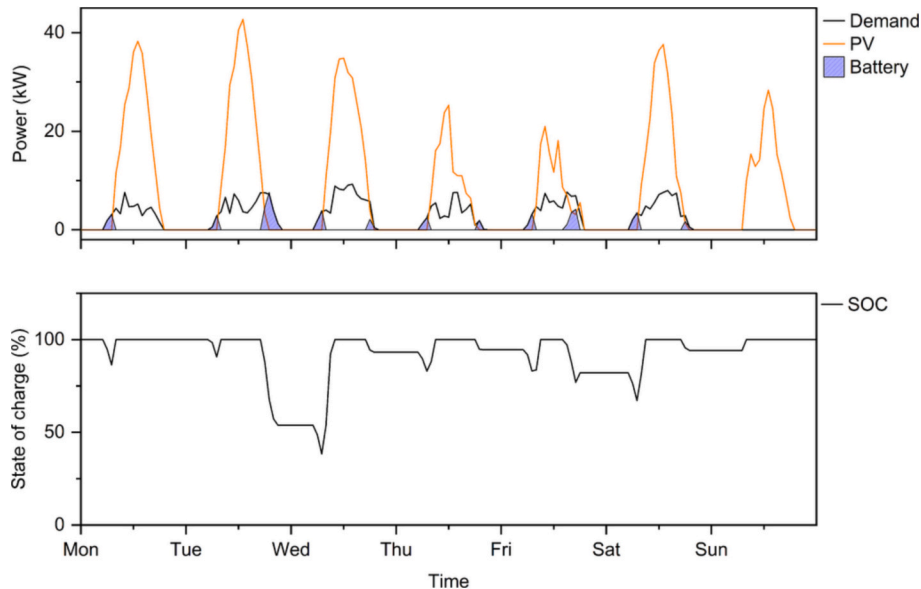


Fig. 12. Power profile of the PV/battery-scenario during one-week of peanut oil production; demand, PV-, and battery power (top), state of charge (SOC) of the battery (bottom).

The NPC would be 50,746 €, with an initial investment of 34,268 € where 13,054 € is for PV and 11,916 € for the battery. The COE would be 0.21 €/kWh, and the energy surplus would be 27,135 kWh/a (66.8 %).

PV/grid-scenario

The PV/grid-scenario is a PV system connected to the grid without battery storage. It runs on solar energy, with all PV production being consumed by the SME and supported by the grid when being required. It consists of 20.0 kW_p of PV fulfilling 77.3 % of the demand. The unmet demand of this scenario would be 0.03 %. Fig. 14 displays a typical week of production under this scenario. In the middle of the day, the PV is able to meet the demand, however a surplus is not exploited. The grid is always called upon at the beginning and end of the day, and on cloudy days when there is insufficient solar radiation (Tuesday to Friday). This scenario is only realistic if the grid is stable, as no alternative is available in the event of an outage. The NPC would be 34,930 € with an initial investment of 16,091 € and an operating cost of 959 €/a, resulting in a COE of 0.14 €/kWh.

PV/battery/grid-scenario

The PV/battery/grid-scenario is a PV/battery system connected to the grid. It operates primarily on solar-generated energy and, if necessary, draws additional power from the grid. The best hybrid solution resulting from the simulation is a 18.6 kW_p grid connected PV system with 16 kWh battery storage. The renewable fraction of this system would be 90.0 %, with an unmet demand of 0.01 %. Fig. 15 displays a typical week of production under this scenario, demonstrating how the grid compensates for low solar radiation. The NPC would be 31,603 € and the initial investment 20,019 € with 9926 € for PV and 4767 € for the battery. The operation cost would be 590 €/a with 370 €/a for grid energy, and the COE of 0.13 €/kWh. The system would produce a surplus of 18,400 kWh/a (58.0 %).

System classification

The optimization results and characteristics of the scenarios presented above are summarized in the Table 7 with the grid only scenario as baseline scenario. The best hybrid scenario proposed is the PV/battery/grid-scenario. It would reduce the NPC from 72,163 € to 31,603 € compared to the baseline scenario. The operating cost would be reduced from 3675 € to 590 €/a, resulting in a COE decrease from 0.29 to 0.13 €/kWh. Under this scenario, the renewable fraction would

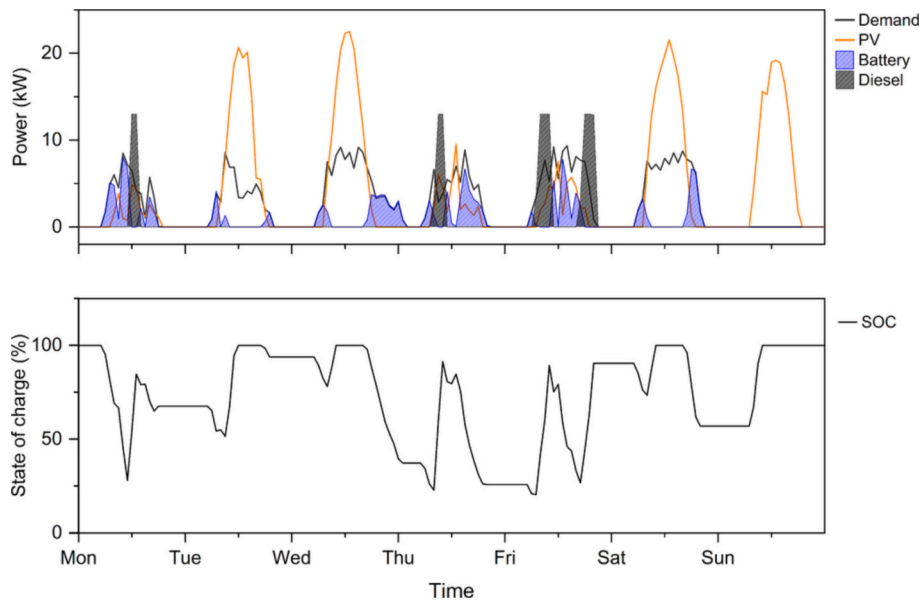


Fig. 13. Power profile of the PV/battery/diesel-scenario during one-week of peanut oil production; demand, PV-, battery- and diesel power (top), state of charge (SOC) of the battery (bottom).

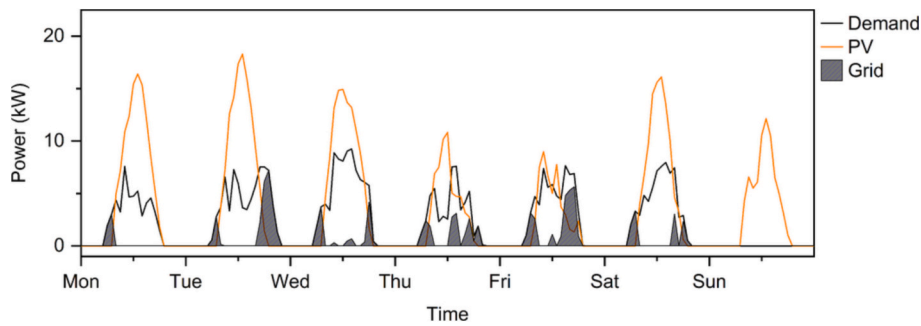


Fig. 14. Power profile of the PV/grid-scenario during one-week of peanut oil production; demand, PV-, grid power.

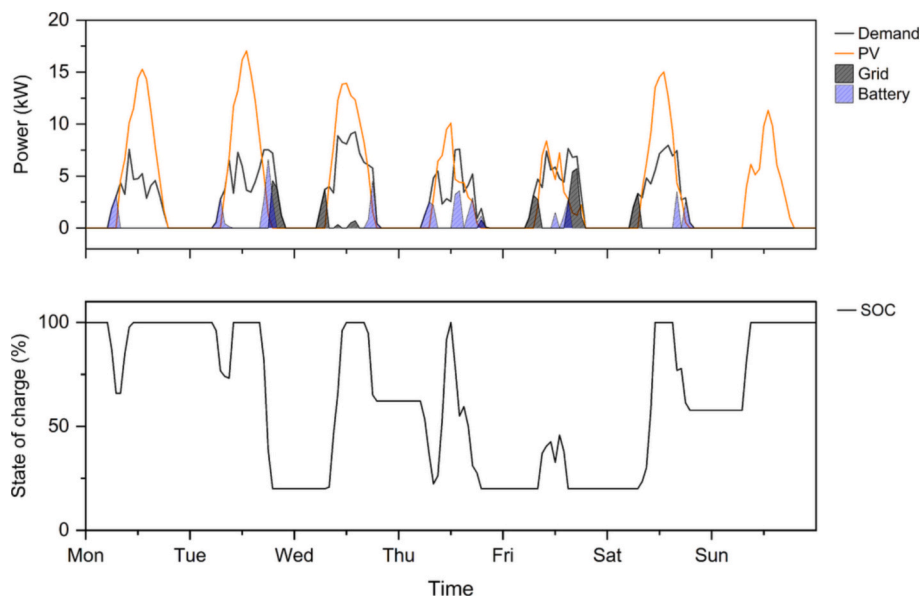


Fig. 15. Power profile of the PV/battery/grid-scenario during one-week of peanut oil production; demand, PV-, battery- and grid power (top), state of charge (SOC) of the battery (bottom).

increase from 0 % to 90.0 %, while the unmet demand would decrease from 0.41 % to 0.01 %. The expected payback period for this scenario is 6.2 years.

For the best off-grid scenario (PV/battery/diesel), allowing to be independent from grid, an initial investment of 34,268 €, would be required, which is 77 % more expensive than the investment of the PV/battery/grid-scenario. This option, as well as the PV/battery-scenario, is not as cost effective as the PV/battery/grid-scenario, but is still more profitable than the grid-scenario.

In Fig. 16 10 out of 14 possible combinations of power sources were ranked according their NPC. The scenario PV-only was not technically feasible and the scenarios diesel-only, PV/diesel, or PV battery/diesel, were exclude from the analysis due to their high NPC, reaching up to 180,000 €. The figure indicates that the PV/battery/grid-scenario is located in position 1. In position 2, the PV/battery/grid/diesel-scenario is similar to the first scenario, since the generator would be rarely used. Scenarios 3 and 4 are PV/grid-scenarios with optional diesel generator (still rarely used). These are options without storage, which means lower initial cost. However, the absence of battery creates a reliability problem with an unstable grid. The optional generator, on the other hand, allows a more stable system. The presented off grid scenarios are the PV/battery/diesel-scenario and the PV/battery-scenario respectively in position 5 and 6 and the grid-scenario is located in position 7. Scenarios 8, 9 and 10 are non-renewable grid systems, with or without diesel and battery. But they remain similar to the baseline, and operate mainly on the grid.

Discussion

The results demonstrate the feasibility of using a production plant diagnosis to create a load profile for sizing a PV system. During the diagnosis, four operations were identified that correspond to a simplified model of the industrial extraction process of peanut oil by cold pressing. The operating parameters differ slightly from the optimal parameters found in the literature. The steamed peanuts are mixed with 15 % of shell while a mixing of 5 to 10 % of shell is recommended (List, 2016). However, it should be noted that a worn screw in the oil press or a poor destoning after shelling may cause clogging in the oil press, requiring more shells to be added. Additionally, the steaming time in this SME goes up to 90 min, whereas the optimum properties reported in the literature suggest a range of 10 to 25 min (Ibrahim & Onwualu, 2005; Sivakumaran et al., 1985; List, 2016). During the steaming in this SME the shells are used as fuel, which makes the operation cost and energy efficient.

The service-oriented mode of operation of the SME led to the definition of parameters to simulate the variability of activities. In the present case study, the parameters considered are used to build a more comprehensive picture of the interactions of the SME and the customers. For comparison with existing literature on methods of load profile generation, we can categorize them into two main groups. The first group comprises non-parametric methods currently employed in industrial load profile generation. These methods utilize typical load profiles (Gouveia & Seixas, 2016; Little & Blanchard, 2022; Sanchez

et al., 2009; Sandhaas et al., 2022), scaling them to fit a given daily consumption. However, these approaches lack the flexibility to simulate various application scenarios, and are confined to specific processes for which they were designed. Notably, the literature lacks a typical rural service-oriented industry profile. The second group is parametric and is more commonly applied in households (Lombardi et al., 2019; Mandelli, Merlo, & Colombo, 2016; Sepehr et al., 2018). In this group, specific parameters are assigned to each equipment, encompassing nominal power, functioning time, and frequency of use. Employing a bottom-up approach, these parameters are used to individually simulate each appliance. In the proposed method, these parameters are expanded by including customer variability and customer acceptance windows. The approach mirrors the parametric method used for households. However, the innovation lies in the focus on customer variability, allowing the entire SME to be simulated instead of defining variability for each appliance. This enables a comprehensive process modeling and preserves the operating ranges of each device. As a result, the realism in capturing the SME's operating modes is improved and additional values such as production capacity and raw material consumption can be taken into account in the simulation.

Similarities were found between peak and average power consumption obtained from simulation and on-site measurements. This validates the model used. The PV/battery/grid-scenario was found to be the most economic solution. It shows a 90.0 % renewable energy coverage at a low storage requirement (20 % of the daily consumption), based on the fact that the activities are mostly performed during the day, with power demands early in the morning from 06:00 and at early night to finish the processing of already started batches. The optimization shows that no new customers should be accepted close to sunset and the end time of customer acceptance was at 16:20.

An alternative conventional sizing approach could be made by considering the typical "commercial load profile" available on HOMER Pro, scaled to the daily energy consumption of the SME. The result would be again a PV/battery/grid-scenario with 35.4 kW_p of PV, 40 kWh battery storage. However, this system based on standard load profiles would be larger than for a real load profile and the investment would be 37,858 €. The proposed approach, therefore, allows a reduction in the investment cost of 47 %, in particular thanks to a reduced storage capacity of 60 %.

In addition, a PV system for the SME would occupy a large part of the estate in terms of solar panels. Some studies suggest limits to the space occupied by hybrid systems (Baruah et al., 2021). Ideally, only the roof of the building should be occupied. This is the case for the PV/battery/grid-scenario, which would occupy only 35 % of the available space (62 % of the roof). However, the PV/battery-scenario would occupy 89 % of the total surface area. This necessitates additional investment in the supporting structure, leading to increased NPC and COE, which has not been considered in our study.

Nevertheless, a large amount of energy remains unused in the hybrid solutions. Alternatives should be found to exploit this extra energy. Since Senegal, for the time being, does not allow a feed-in to the grid, an additional economic activity for using the excess energy should be developed. The company already possesses other equipment, such as a

Table 7
Parameters of the investigated scenarios, ranked according net present cost (NPC).

Scenarios	PV	Battery capacity	NPC	Initial cost	COE	Ren. fraction	Unmet demand	Total energy produced	Total energy consumption	Excess electricity
	(kW _p)	(kWh)	(€)	(€)	(€)	(%)	(%)	(kWh/a)	(kWh/a)	(kWh/a)
Grid	–	–	72,163	0	0.29	0	0.41	12,504	12,504	0
PV/battery	46.6	40	54,958	45,323	0.22	100	0.36	76,298	12,510	62,961
PV/battery/diesel	24.5	40	50,746	34,268	0.21	95.9	0	40,603	12,555	27,135
PV/grid	20.0	–	34,930	16,091	0.14	77.3	0.31	35,548	12,551	22,486
PV/battery/grid	18.6	16	31,603	20,019	0.13	90.0	0.01	31,742	12,554	18,400

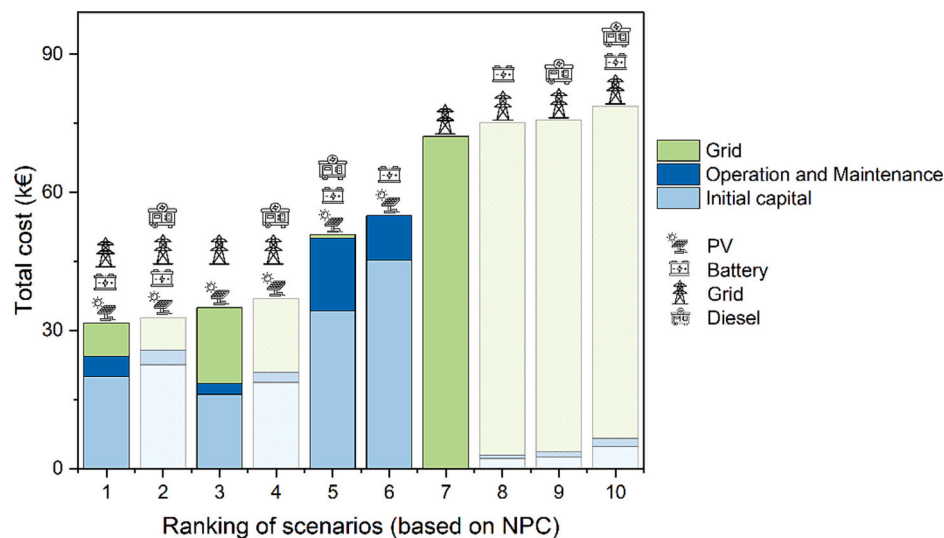


Fig. 16. Classification of power supply scenarios ranked according to total cost for 25 years of operation.

rice huller, which could serve as a viable alternative during the off-season of peanut oil production. [Bhayo et al. \(2019\)](#) evaluated PV system performance for households and suggested using excess energy to power a pumping system. This option is intriguing, especially since the company has a water well. However, the capacity of a household pumping system alone may not fully utilize the surplus. Another viable option is redirecting the excess energy to support a nearby irrigation system. A similar approach was adopted by [Chowdhury et al. \(2015\)](#), in rural Bangladesh, where a mini-grid powered households and surplus energy were utilized to operate irrigation pumps.

Conclusions

In this study, a novel process simulation model was developed to obtain load profiles for PV sizing. The model focuses on capturing the complex peanut oil production system of SME and service-based operation, where various machines operate at different times throughout the day, based on the operation strategy and the customers demand. The peanut oil production process was characterized by a mass balance, utilizing a bottom-up approach that considers customer variability. An implementation in MATLAB Simulink involved adjusting the model's operating parameters to align with real on-site conditions, aiming for a daily production of 4 tons and an average consumption of 67 kWh. The load profile was then compared to on-site measurements, revealing a 7.07 % error, affirming its validity for solar system sizing.

The load profiles were used in HOMER Pro to find the optimal configurations from an economic point of view. All the hybrid configurations combining grid, PV, battery, and diesel generator were evaluated. The results showed that the most economical solution is a PV/battery/grid-system with 18.6 kW_p of PV and 16 kWh of battery storage. The NPC would be 31,603 € with initial costs of 20,019 € and the COE would be 0.13 €/kWh. The renewable fraction of the suggested PV system is 90.0 % with an unmet load of 0.01 %. The payback period of the system would be 6.2 years.

For an off-grid solution, the simulations showed that although the solutions are more cost-effective than the grid, the benefits are lower than that of the hybrid solution and the investment costs are very high. The COE of the fully renewable PV/battery-system would be 0.22 €/kWh, which is still lower than the COE of energy from the grid at 0.29 €/kWh. However, this scenario would be not affected by rising electricity prices and could be applied in remote areas without grid

connection.

Beyond the load profiles established and used for the simulations, it should be noted that the SME may have other parallel activities, such as rice husking. Excess energy may be used for those activities. An analysis of the whole activity of the SME could show how much of the parallel activities can be covered by the PV system.

CRediT authorship contribution statement

Wiomou Joévin Bonzi: Conceptualization, Methodology, Software, Validation, Formal analysis, Investigation, Writing – original draft, Visualization. **Sebastian Romuli:** Conceptualization, Methodology, Investigation, Writing – review & editing, Visualization, Supervision, Project administration, Funding acquisition. **Djicknoum Diouf:** Conceptualization, Investigation, Resources, Writing – review & editing, Supervision. **Bruno Piriou:** Conceptualization, Investigation, Writing – review & editing. **Klaus Meissner:** Writing – review & editing, Supervision, Project administration, Funding acquisition. **Joachim Müller:** Conceptualization, Methodology, Resources, Writing – review & editing, Supervision, Project administration, Funding acquisition.

Declaration of competing interest

The authors declare the following financial interests/personal relationships which may be considered as potential competing interests: Wiomou Joevin Bonzi reports financial support was provided by German Academic Exchange Service. Wiomou Joevin Bonzi reports financial support, equipment, drugs, or supplies, and travel were provided by European Union.

Acknowledgements

We would like to acknowledge the contributions of the **BIOSTAR project** “Bioenergy for SMEs in West Africa”: FOOD/2019/410-794 - funded by the European Union and Agence Française de Développement (AFD) as part of the DeSIRA program, which provided the framework and support necessary for the research presented in this article. We would also like to express our gratitude to the German Academic Exchange Service (**DAAD**) for the scholarship awarded to the first author of this article. Finally, we would like to thank **Moussa Niang** for his contributions to the diagnosis phase of this study.

Appendix A

Nomenclature

Symbols

CAI_i : customer arrival indicator
 $C_{k,i}$: command from the operation strategy
 E : total energy consumption of the SME, Wh
 Eff_k : operation yield, kg/kg
 m_i : mass of the receipted in-shell peanut in the SME, kg
 min : minute
 N : number of centroids in the k-means clustering classification
 n_i : order size of in-shell peanut, 50-kg-bags
 n_{max} : maximum order size of in-shell peanut, 50-kg-bags
 P : probability
 P_{FP} : electrical power of filter press, W
 P_{Oil} : electrical power of oil press, W
 P_{Sh} : electrical power of sheller, W
 p_c : customer arrival probability
 P_k : averaged electrical power of the operation k engine, W
 $P_{k,i}$: instant power of the operation k at time step i, W
 $P_{measured, average}$: average power of the measured load, W
 $P_{measured,x}$: centroid of the measured load profile, W
 $P_{model,x}$: centroid of the simulation load profile, W
 P_{peak} : daily peak power, W
 r : peak to average power ratio, W/W
 $S_{k,i}$: stored material from the operation k-1, kg
 T : duration of the simulation, min
 T_{end} : time at which the SME stops accepting customers
 $TPFP$: throughput of filter press, kg/min
 TP_k : average throughput of processed material of operation k, kg/min
 $TP_{k,i}$: throughput of processed material of operation k at a time step i, kg/min
 $TPOil$: throughput of oil press, kg/min
 TPS : throughput of steamer, kg/min
 $TPSh$: throughput of sheller, kg/min
 T_{start} : time at which the SME begins accepting customers
 T_{start_k} : time at which the SME start operation

Subscript

i : time step, minute
 k : operation of the process
 x : centroid index

Abbreviation

ANN: Artificial Neural Network
 AC: Alternating Current, A
 CCS: Cycle Charging Strategy
 COE: Cost of Energy, €/kWh
 DC: Direct Current, A
 HOMER Hybrid Optimization Model for Electric Renewables
 INSEL: INtegrated Simulation Environment Language
 LF: Load Factor
 LFS: Load Following Strategy
 MATLAB: MATrix LABoratory
 MPPT: Maximum Power Point Tracking
 NASA: National Aeronautics and Space Administration
 NPC: Net Present Cost, €
 NRMSE: Normalised Root-Mean-Squared Error, %
 O&M: Operation and Maintenance
 PP: Peak Power
 PV: Photovoltaics
 RMSE: Root Mean Square Error
 SAS: Statistical Analysis System
 SME: Small and medium-sized enterprise
 SOC: State of Charge, %

Appendix B

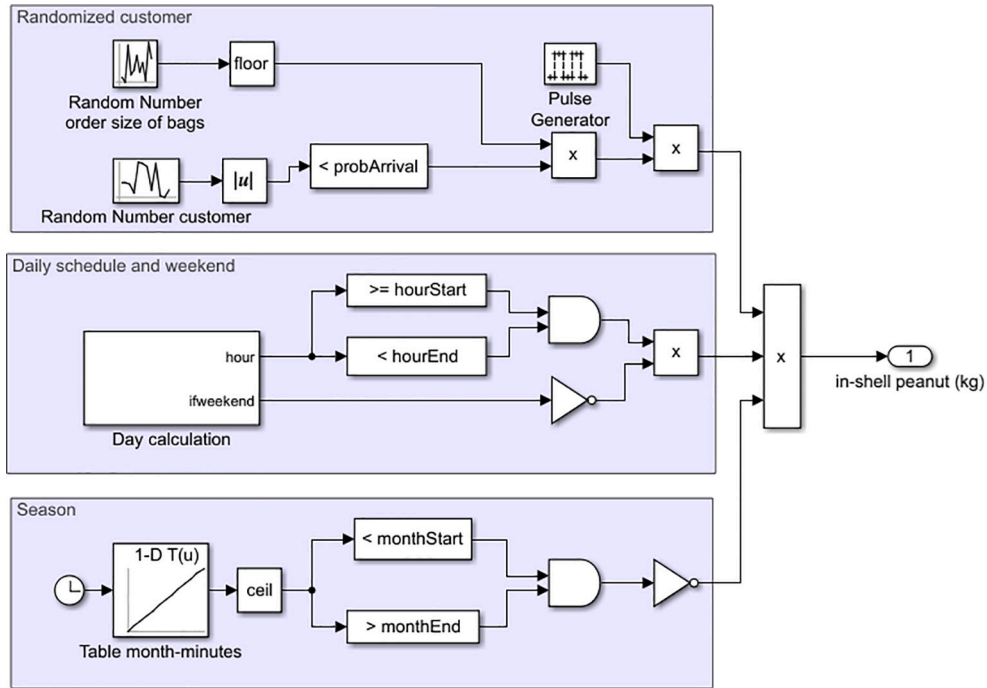


Fig. B.1. Simulink block model of in-shell peanuts, defined based on the randomly arriving customers, the daily schedule and the months defining the production season during the year.

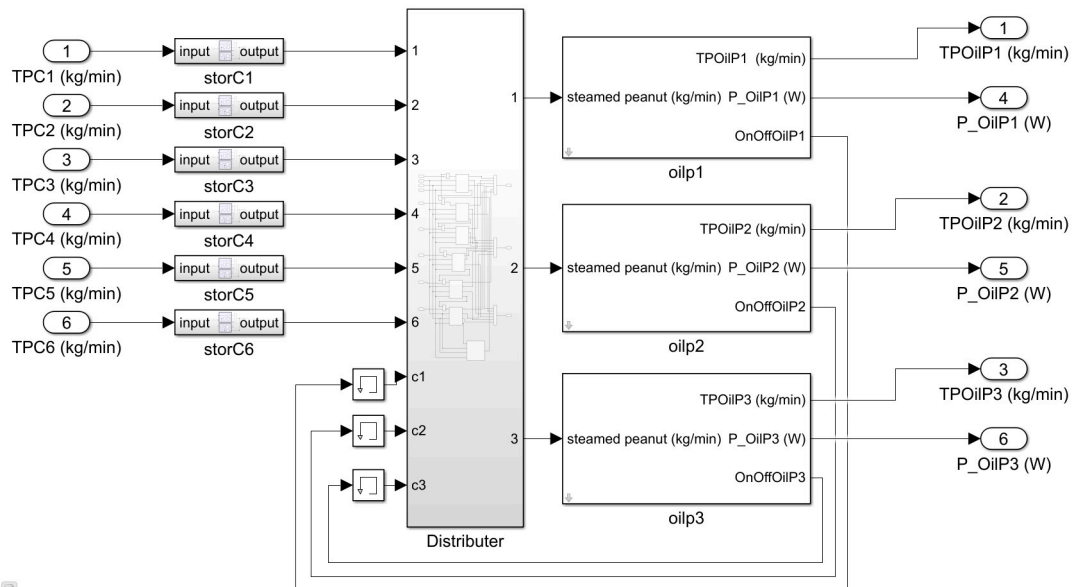


Fig. B.2. Simulink block model of oil pressing with the same configuration as shelling, steaming and filtration block. The block receives input from the throughput of the six different steamers and the input is stored in the intermediate storage before going to the distributor which will allocate the input to one available oil press.

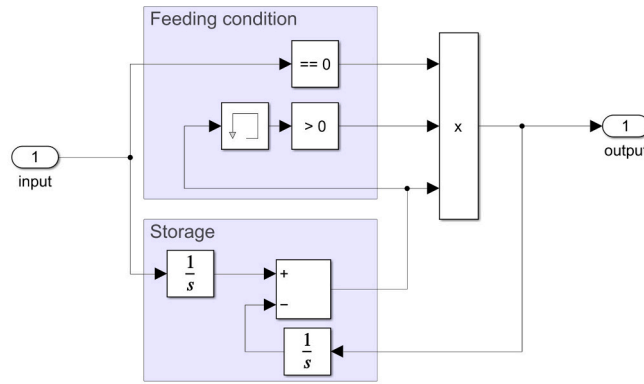


Fig. B.3. Simulink block model of intermediary storage which accumulates throughputs until the end of the previous operation. Once a steaming operation is finished, the integral of the throughput is sent to the distributor block.

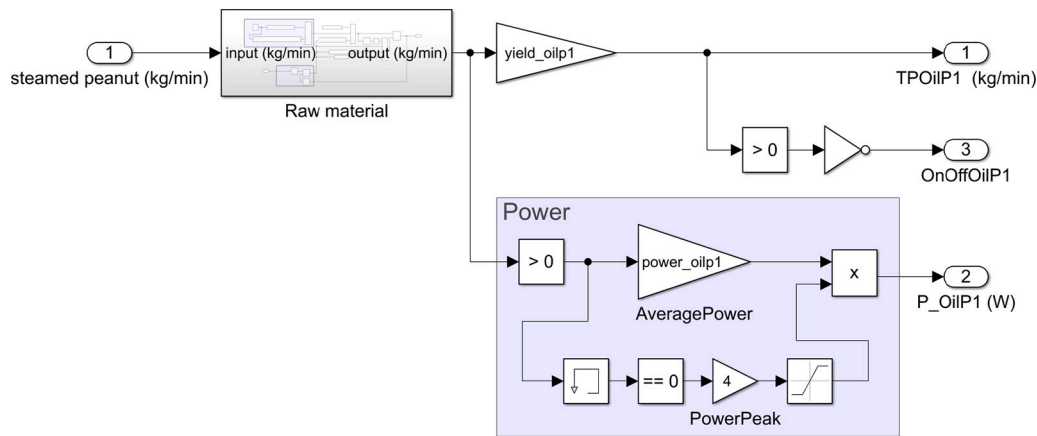


Fig. B.4. Simulink block model of oil press which multiply the raw material by the operation yield, and in parallel, monitors the electrical power of the operation.

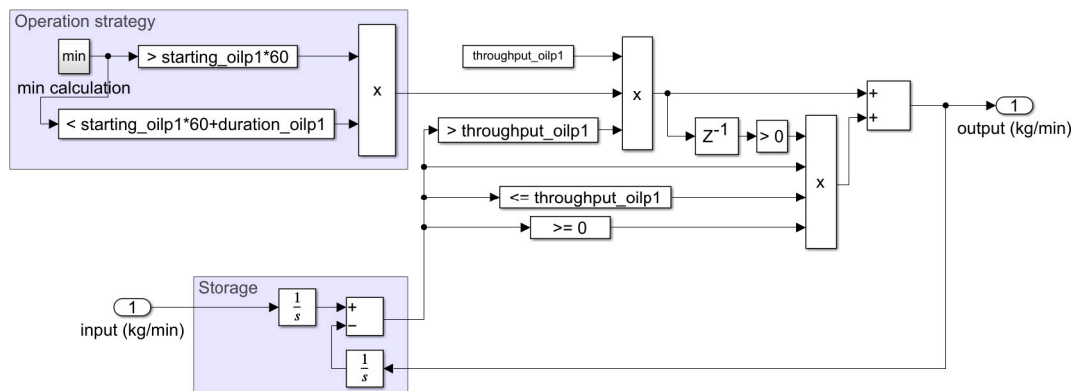


Fig. B.5. Simulink block model of raw material in the oil press block, which acts as a buffer and deducts the raw material based on the operation throughput.

References

Abarkan, M., Errahimi, F., M'Sirdi, N. K., & Naamane, A. (2013). Analysis of energy consumption for a building using wind and solar energy sources. *Energy Procedia*, 42, 567–576. <https://doi.org/10.1016/j.egypro.2013.11.058>

Alsadi, S., & Khatib, T. (2018). Photovoltaic power systems optimization research status: A review of criteria, constrains, models, techniques, and software tools. *Applied Sciences (Switzerland)*, 8(10). <https://doi.org/10.3390/app8101761>

Anoune, K., Lakhnizi, A., Bouya, M., Astito, A., & Ben Abdellah, A. (2018). Sizing a PV-Wind based hybrid system using deterministic approach. *Energy Conversion and Management*, 169, 137–148. <https://doi.org/10.1016/j.enconman.2018.05.034>

Awan, M. M. A., Javed, M. Y., Asghar, A. B., Ejsmont, K., & Zia-Ur-rehman. (2022). Economic integration of renewable and conventional power sources—A case study. *Energies*, 15(6). <https://doi.org/10.3390/en15062141>

Azad, S. A., Ali, A. B. M. S., & Wolfs, P. (2014). Identification of typical load profiles using K-means clustering algorithm. *Asia-Pacific World Congress on Computer Science and Engineering*, 1–6. <https://doi.org/10.1109/APWCCSE.2014.7053855>

Barra, L., Catalanotti, S., Fontana, F., & Lavorante, F. (1984). An analytical method to determine the optimal size of a photovoltaic plant. *Solar Energy*, 33(6), 509–514. [https://doi.org/10.1016/0038-092X\(84\)90005-7](https://doi.org/10.1016/0038-092X(84)90005-7)

Baruah, A., Basu, M., & Amuley, D. (2021). Modeling of an autonomous hybrid renewable energy system for electrification of a township: A case study for Sikkim, India. *Renewable and Sustainable Energy Reviews*, 135, Article 110158. <https://doi.org/10.1016/j.rser.2020.110158>

Bhayo, B. A., Al-Kayiem, H. H., & Gilani, S. I. (2019). Assessment of standalone solar PV-Battery system for electricity generation and utilization of excess power for water pumping. *Solar Energy*, 194, 766–776. <https://doi.org/10.1016/j.solener.2019.11.026>

- Bimbenyimana, S., Asemota, G. N. O., & Ihrwe, P. J. (2018). Optimization comparison of stand-alone and grid-tied solar PV systems in Rwanda. *OALib*, 05(05), 1–18. <https://doi.org/10.4236/oalib.1104603>
- Bimbenyimana, S., Asemota, G. N. O., Niyonteze, J. D. D., Nsengimana, C., Ihrwe, P. J., & Li, L. (2019). Photovoltaic solar technologies: Solution to affordable, sustainable, and reliable energy access for all in Rwanda. *International Journal of Photoenergy*, 2019. <https://doi.org/10.1155/2019/5984206>
- Blodgett, C., Dauenhauer, P., Louie, H., & Kickham, L. (2017). Accuracy of energy-use surveys in predicting rural mini-grid user consumption. *Energy for Sustainable Development*, 41, 88–105. <https://doi.org/10.1016/j.esd.2017.08.002>
- CEN/TS 14774-3:2004. (2004). *Determination of moisture content-oven dry method*.
- Chowdhury, S. A., Aziz, S., Groh, S., Kirchoff, H., & Leal Filho, W. (2015). Off-grid rural area electrification through solar-diesel hybrid minigrids in Bangladesh: Resource-efficient design principles in practice. *Journal of Cleaner Production*, 95, 194–202. <https://doi.org/10.1016/j.jclepro.2015.02.062>
- Chuan, L., & Ukil, A. (2015). Modeling and validation of electrical load profiling in residential buildings in Singapore. *IEEE Transactions on Power Systems*, 30(5), 2800–2809. <https://doi.org/10.1109/TPWRS.2014.2367509>
- DGF-Einheitsmethoden. (2006). *Deutsche Einheitsmethoden zur Untersuchung von Fetten, Fettprodukten, Tensiden und verwandten Stoffen*.
- Duma, T., Seteni, B., & Dzobo, O. (2023). *Techno-economic analysis of solar-PV/battery system for a foundry company*. Proceedings of the 31st Southern African Universities Power Engineering Conference, SAUPEC 2023. <https://doi.org/10.1109/SAUPEC57889.2023.10057896>.
- Eales, A., Buckland, H., Frame, D., Unyolo, B., Gondwe, C., & Kaunda, M. (2017). Productive use of solar PV in rural Malawi: Feasibility studies. <https://strathprints.strath.ac.uk/id/eprint/60948>.
- Gelchu, M. A., Ehnberg, J., Shiferaw, D., & Ahlgren, E. O. (2023). Impact of demand-side management on the sizing of autonomous solar PV-based mini-grids. *Energy*, 278. <https://doi.org/10.1016/j.energy.2023.127884>
- Gouveia, J. P., & Seixas, J. (2016). Unraveling electricity consumption profiles in households through clusters: Combining smart meters and door-to-door surveys. *Energy and Buildings*, 116, 666–676. <https://doi.org/10.1016/j.enbuild.2016.01.043>
- Green, M. A. (2019). How did solar cells get so cheap?. In , 3. *Joule* (pp. 631–633). Cell Press. <https://doi.org/10.1016/j.joule.2019.02.010>. Issue 3.
- Halabi, L. M., Mekhilef, S., Olatomiwa, L., & Hazelton, J. (2017). Performance analysis of hybrid PV/diesel/battery system using HOMER: A case study Sabah, Malaysia. *Energy Conversion and Management*, 144, 322–339. <https://doi.org/10.1016/j.enconman.2017.04.070>
- Harish, V. S. K. V., Anwer, N., & Kumar, A. (2022). Applications, planning and socio-techno-economic analysis of distributed energy systems for rural electrification in India and other countries: A review. *Sustainable Energy Technologies and Assessments*, 52. <https://doi.org/10.1016/j.seta.2022.102032>
- Hernández-Callejo, L., Gallardo-Saavedra, S., & Alonso-Gómez, V. (2019). A review of photovoltaic systems: Design, operation and maintenance. In , Vol. 188. *Solar Energy* (pp. 426–440). Elsevier Ltd.. <https://doi.org/10.1016/j.solener.2019.06.017>
- Ibrahim, A., & Onwuwalu, A. P. (2005). Technologies for extraction of oil from oil-bearing agricultural products: A review. *Journal of Agricultural Engineering and Technology (JAET)*, 13, 58–89. <https://nairametrics.com/wp-content/uploads/2013/02/technology-of-extracting-oil-from-the-oil-bearing.pdf>.
- Ikotun, A. M., Ezugwu, A. E., Abualigah, L., Abuhaija, B., & Heming, J. (2023). K-means clustering algorithms: A comprehensive review, variants analysis, and advances in the era of big data. *Information Sciences*, 622, 178–210. <https://doi.org/10.1016/j.ins.2022.11.139>
- Kaygusuz, K. (2012). Energy for sustainable development: A case of developing countries. *Renewable and Sustainable Energy Reviews*, 16(2), 1116–1126. <https://doi.org/10.1016/j.rser.2011.11.013>
- Khatib, T., Ibrahim, I. A., & Mohamed, A. (2016). A review on sizing methodologies of photovoltaic array and storage battery in a standalone photovoltaic system. In , Vol. 120. *Energy Conversion and Management* (pp. 430–448). Elsevier Ltd.. <https://doi.org/10.1016/j.enconman.2016.05.011>
- Kumra, A., Kumar Gaur, M., & Malvi, C. (2012). Sizing of a standalone photovoltaic system for small scale industry. *International Journal of Emerging Technology and Advanced Engineering*, 8(20), 65–69. www.ijetae.com.
- Lalwani, M., Kothari, D. P., & Singh, M. (2010). Investigation of solar photovoltaic simulation softwares. *International Journal of Applied Engineering Research, Dindigul*, 1(3), 585–601.
- Lambert, T., Gilman, P., & Lilienthal, P. (2005). Micropower system modeling with homer. In *Integration of alternative sources of energy* (pp. 379–418). Wiley. <https://doi.org/10.1002/0471755621.ch15>
- Lighting Global. (2019). The market opportunity for Productive Use Leveraging Solar Energy (PULSE) in Sub-Saharan Africa. <https://www.lightingglobal.org/wp-content/uploads/2022/04/PULSE-Report.pdf>.
- List, G. R. (2016). Processing and food uses of peanut oil and protein. In *Peanuts: Genetics, processing, and utilization* (pp. 405–428). Elsevier Inc.. <https://doi.org/10.1016/B978-1-63067-038-2.00015-0>
- Little, M., & Blanchard, R. (2022). Pre-feasibility methodology to compare productive uses of energy supplied by stand-alone solar photovoltaic systems: A Tanzanian case study. *Energy for Sustainable Development*, 70, 497–510. <https://doi.org/10.1016/j.esd.2022.08.018>
- Lombardi, F., Balderrama, S., Quoilin, S., & Colombo, E. (2019). Generating high-resolution multi-energy load profiles for remote areas with an open-source stochastic model. *Energy*, 177, 433–444. <https://doi.org/10.1016/j.energy.2019.04.097>
- Lorenzoni, L., Cherubini, P., Fioriti, D., Poli, D., Micangeli, A., & Giglioli, R. (2020). Classification and modeling of load profiles of isolated mini-grids in developing countries: A data-driven approach. *Energy for Sustainable Development*, 59, 208–225. <https://doi.org/10.1016/j.esd.2020.10.001>
- Ma, T., Yang, H., & Lu, L. (2014). Solar photovoltaic system modeling and performance prediction. In , Vol. 36. *Renewable and sustainable energy reviews* (pp. 304–315). Elsevier Ltd.. <https://doi.org/10.1016/j.rser.2014.04.057>
- Maghraby, H. A. M., Shwehdi, M. H., & Al-Bassam, G. K. (2002). Probabilistic assessment of photovoltaic (PV) generation systems. *IEEE Transactions on Power Systems*, 17(1), 205–208. <https://doi.org/10.1109/59.982215>
- Makkiabadi, M., Hoseinzadeh, S., Taghavi-rashidzadeh, A., Soleimanezhad, M., Kamyabi, M., Hajabdollahi, H., ... Piras, G. (2021). Performance evaluation of solar power plants: A review and a case study. In , Vol. 9. *Processes*. MDPI. <https://doi.org/10.3390/pr9122253>. Issue 12.
- Mandelli, S., Barbieri, J., Mereu, R., & Colombo, E. (2016). Off-grid systems for rural electrification in developing countries: Definitions, classification and a comprehensive literature review. In , Vol. 58. *Renewable and Sustainable Energy Reviews* (pp. 1621–1646). Elsevier Ltd.. <https://doi.org/10.1016/j.rser.2015.12.338>
- Mandelli, S., Brivio, C., Colombo, E., & Merlo, M. (2016). A sizing methodology based on Levelized Cost of Supplied and Lost Energy for off-grid rural electrification systems. *Renewable Energy*, 89, 475–488. <https://doi.org/10.1016/j.renene.2015.12.032>
- Mandelli, S., Merlo, M., & Colombo, E. (2016). Novel procedure to formulate load profiles for off-grid rural areas. *Energy for Sustainable Development*, 31, 130–142. <https://doi.org/10.1016/j.esd.2016.01.005>
- Mathew, M., Hossain, M. S., Saha, S., Mondal, S., & Haque, M. E. (2022). Sizing approaches for solar photovoltaic-based microgrids: A comprehensive review. In , Vol. 4. *IET Energy Systems Integration* (pp. 1–27). John Wiley and Sons Inc.. <https://doi.org/10.1049/esi2.12048>. Issue 1.
- Mellit, A. (2007). Sizing of photovoltaic systems: A review. In , Vol. 10. *Revue des Energies Renouvelables*. <https://api.semanticscholar.org/CorpusID:17125857>
- Mellit, A., Kalogirou, S. A., Hontoria, L., & Shaari, S. (2009). Artificial intelligence techniques for sizing photovoltaic systems: A review. *Renewable and Sustainable Energy Reviews*, 13(2), 406–419. <https://doi.org/10.1016/j.rser.2008.01.006>
- Ogumike, C., Modibbo, A., & Denai, M. (2013). Optimized residential loads scheduling based on dynamic pricing of electricity: A simulation study. In *3rd solar integration workshop*. <https://www.researchgate.net/publication/332320130>.
- Olk, H., & Mundt, J. (2016). Photovoltaics for productive use applications: A catalogue of DC-appliances. <https://d-nb.info/1127676040/34>.
- Oviroh, P. O., & Jen, T. C. (2018). The energy cost analysis of hybrid systems and diesel generators in powering selected base transceiver station locations in Nigeria. *Energies*, 11(3), 7–9. <https://doi.org/10.3390/en11030687>
- Parida, B., Iniyuan, S., & Goic, R. (2011). A review of solar photovoltaic technologies. *Renewable and Sustainable Energy Reviews*, 15(3), 1625–1636. <https://doi.org/10.1016/j.rser.2010.11.032>
- Rajesh, R., & Carolin Mabel, M. (2015). A comprehensive review of photovoltaic systems. In , Vol. 51. *Renewable and sustainable energy reviews* (pp. 231–248). Elsevier Ltd.. <https://doi.org/10.1016/j.rser.2015.06.006>
- Rodrigues, F., Cardeira, C., & Calado, J. M. F. (2014). The daily and hourly energy consumption and load forecasting using artificial neural network method: A case study using a set of 93 households in Portugal. *Energy Procedia*, 62, 220–229. <https://doi.org/10.1016/j.egypro.2014.12.383>
- Sadio, A., Mbodji, S., & Fall, I. (2018). New numerical sizing approach of a standalone photovoltaic power at Ngoundiane, Senegal. *EAI Endorsed Transactions on Energy Web*, 5(16), Article 153814. <https://doi.org/10.4108/eai.30-1-2018.153814>
- Salehin, S., Ferdaous, M. T., Chowdhury, R. M., Shithi, S. S., Rofi, M. S. R. B., & Mohammed, M. A. (2016). Assessment of renewable energy systems combining techno-economic optimization with energy scenario analysis. *Energy*, 112, 729–741. <https://doi.org/10.1016/j.energy.2016.06.110>
- Sanchez, I. B., Espinosa, I. D., Moreno Sarrion, L., Lopez, A. Q., & Burgos, I. N. (2009). Clients segmentation according to their domestic energy consumption by the use of self-organizing maps. In *2009 6th International Conference on the European Energy Market* (pp. 1–6). <https://doi.org/10.1109/EEM.2009.5207172>
- Sandhaas, A., Kim, H., & Hartmann, N. (2022). Methodology for generating synthetic load profiles for different industry types. *Energies*, 15(10). <https://doi.org/10.3390/en15103683>
- Senthil Kumar, R., Puja Priyadarshini, N., & Natarajan, E. (2015). Experimental and Numerical Analysis of Photovoltaic Solar Panel using Thermoelectric Cooling. *Indian Journal of Science and Technology*, 8(36). <https://doi.org/10.17485/ijst/2015/v8i36/87646>
- Sepehr, M., Eghtedaei, R., Toolabimoghadam, A., Noorollahi, Y., & Mohammadi, M. (2018). Modeling the electrical energy consumption profile for residential buildings in Iran. *Sustainable Cities and Society*, 41(May), 481–489. <https://doi.org/10.1016/j.scs.2018.05.041>
- Serrano-Guerrero, X., Escrivá-Escrivá, G., & Roldán-Blay, C. (2018). Statistical methodology to assess changes in the electrical consumption profile of buildings. *Energy and Buildings*, 164, 99–108. <https://doi.org/10.1016/j.enbuild.2017.12.059>
- Sivakumaran, K., Goodrum, John W., & Bradley, Ralph A. (1985). Expeller optimization for peanut oil production. *Transactions of the ASAE*, 28(1), 316–320. <https://doi.org/10.13031/2013.32249>
- The World Bank. (2019). *Getting electricity: System average interruption duration index (SAIDI)*. GovData360. https://govdata360.worldbank.org/indicators/h2d96dbda?country=SEN&indicator=42570&viz=line_chart&years=2014,2019
- Thomas, J. S., John, J., Sajji, N., Sunny, N. M., Krishnan, A., & Mathew, T. (2014). Design and financial analysis of a micro grid-tie solar PV system for a small scale industry in Kerala. In *2014 International Conference on Green Computing Communication and Electrical Engineering (ICGCCCE)* (pp. 1–5). <https://doi.org/10.1109/ICGCCCE.2014.6922464>

- Tso, G. K. F., & Yau, K. K. W. (2007). Predicting electricity energy consumption: A comparison of regression analysis, decision tree and neural networks. *Energy*, 32(9), 1761–1768. <https://doi.org/10.1016/j.energy.2006.11.010>
- Vu, B. H., & Chung, I. Y. (2022). Optimal generation scheduling and operating reserve management for PV generation using RNN-based forecasting models for stand-alone microgrids. *Renewable Energy*, 195, 1137–1154. <https://doi.org/10.1016/j.renene.2022.06.086>
- Wassie, Y. T., & Ahlgren, E. O. (2023). Performance and reliability analysis of an off-grid PV mini-grid system in rural tropical Africa: A case study in southern Ethiopia. *Development Engineering*, 8. <https://doi.org/10.1016/j.deveng.2022.100106>
- Wijaya, M. E., & Tezuka, T. (2013). A comparative study of households' electricity consumption characteristics in Indonesia: A techno-socioeconomic analysis. *Energy for Sustainable Development*, 17(6), 596–604. <https://doi.org/10.1016/j.esd.2013.09.004>
- Zhang, G., Li, Y., & Deng, X. (2020). K-means clustering-based electrical equipment identification for smart building application. *Information*, 11(1), 27. <https://doi.org/10.3390/info11010027>
- Zhang, T., Chandler, W. S., Hoell, J. M., Westberg, D., Whitlock, C. H., & Stackhouse, P. W. (2008). A global perspective on renewable energy resources: Nasa's prediction of worldwide energy resources (power) project. In , Vol. I–Vol. V. *Proceedings of ISES World Congress 2007* (pp. 2636–2640). Berlin Heidelberg: Springer. https://doi.org/10.1007/978-3-540-75997-3_532.